JOURNAL OF SPACECRAFT AND ROCKETS
Vol. 46, No. 2, March–April 2009

Lenticular Jointed Antenna Deployment Anomaly and Resolution Onboard the Mars Express Spacecraft

Douglas S. Adams*
Jet Propulsion Laboratory, California Institute of Technology, Pasadena, California 91109
and
Mehran Mobrem†
Northrop Grumman Space Technology Astro Aerospace, Carpinteria, California 93013

DOI: 10.2514/1.36891

During the summer of 2005, ESA deployed a series of three lenticular jointed antenna booms that formed a first-of-its-kind ground-penetrating radar antenna onboard the Mars Express spacecraft. The booms were each released from their cradles with a high level of stored energy and allowed to deploy in a chaotic manner with no direct control over their speed or range of motion until their final geometries were achieved. Despite careful preparations, an unforeseen anomaly occurred during the release of the first boom that resulted in a partially deployed state. The flight team was able to determine the boom's intermediate geometry with a high degree of accuracy and to recommend a corrective spacecraft maneuver. This determination, the measured boom properties, and the on-orbit environment that led to the irregularity are discussed, along with the subsequent resolution of the situation and the ultimately successful deployment. Experience gained from the first boom was used to develop a new spacecraft maneuver that was designed to mitigate the chances of another anomaly occurring during the deployment of the second boom, which took place successfully several weeks later. These activities are summarized and the resulting flight data are presented for both dipole booms, which demonstrate a fully deployed and healthy antenna.

Nomenclature

f	=	frequency, Hz
I_{ij}	=	spacecraft mass moment of inertia, kg · m^2
ζ	=	critical damping ratio
$\omega_{x,y,z}$	=	spacecraft angular velocity about the x, y, and z axes, rad/s

I. Introduction

THE Mars Advanced Radar for Subsurface and Ionospheric Sounding (MARSIS) instrument is one of seven payloads onboard ESA's Mars Express spacecraft that launched on 2 June 2003, and entered Mars orbit on 25 December 2003. MARSIS is a long wavelength radar sounder that is designed both to search for evidence of subsurface water and to perform measurements on the Martian ionosphere [1]. When it was commissioned in the summer of 2005, MARSIS became the first ground penetrating radar ever to be used in the study of any body outside of the Earth–moon system.

The antennas for the MARSIS instrument were developed and built by Northrop Grumman Space Technology (NGST) Astro Aerospace. The structural components of the antennas are made up of three foldable flattenable tubes (FFT)^{TM}, whereas the actual conducting antennas are pairs of 22 gauge wires that run inside and along the length of all three booms. The FFT booms are constructed from Kevlar® and fiberglass composite tubes with periodic lenticular hinges that are formed by removing some material from opposing sides of the boom to form slots. Thus, each boom is a single piece structure in its deployed state with all joints fastened and bonded before launch. The booms can be folded elastically at the lenticular hinge locations with no permanent deformation, allowing for very compact storage. Once they are folded, the booms are then compressed accordion style into a cradle for launch and the journey to Mars, as shown in Fig. 1.

The booms are ultimately deployed in a dynamic fashion by sequentially opening a series of cradle doors, thus releasing the stored compression energy and allowing the booms to return to their original prelaunch geometry. In its fully deployed configuration, two of the 20-m MARSIS booms form a 40-m dipole antenna, with the third boom acting as a 7-m monopole antenna. The two dipole booms are the longest known lenticular hinged structures with the largest number of serially deployed hinges ever flown and deployed in space. The deployed dipole and monopole antenna configuration is illustrated along with the Mars Express spacecraft in Fig. 2.

This paper chronicles the resolution of an anomaly that occurred in the flight deployment of the first of the three MARSIS antenna booms, where one of the boom hinges did not fully lock into place during the initial boom release. A short summary of some of the events following the deployment is presented, as well as some of the information used to determine a course of action for the remaining two lenticular booms. Some comparisons are made between finite element modeling results and flight telemetry data to demonstrate the understanding of the state of the partially deployed boom. Results from the accompanying thermal analysis of the hinge are discussed and shown to support the geometry estimated from the flexible modes and spacecraft inertia measurements. The spacecraft maneuver used to warm the stalled hinge is described, along with the subsequent maneuver used to mitigate the chances of a stall occurring during release of the second dipole boom. Special attention is given to the preparation for the maneuvers and the basis for the decisions that led to their selection. This is intended to provide a reference for future missions that may employ a similar deployment technology and would benefit from the experience gained on MARSIS. Final flight data are presented from both dipole boom deployments indicating a correctly deployed and healthy suite of antennas. The monopole's initial deployment was detected, but the final state of the boom is unknown.

Presented as Paper 1684 at the 47th AIAA/ASME/ASCE/AHS/ASC Structures, Structural Dynamics, and Materials Conference, 14th AIAA/ASME/AHS Adaptive Structures Conference, Newport, RI, 1–4 May 2006; received 28 January 2008; revision received 19 August 2008; accepted for publication 21 September 2008.

*Senior Engineer, Spacecraft Structures and Dynamics Group, 4800 Oak Grove Drive. Member AIAA.
†Chief Analyst, Engineering, 6384 Via Real. Member AIAA.

Fig. 1 Stowed MARSIS antenna FFT booms and cradle before launch.

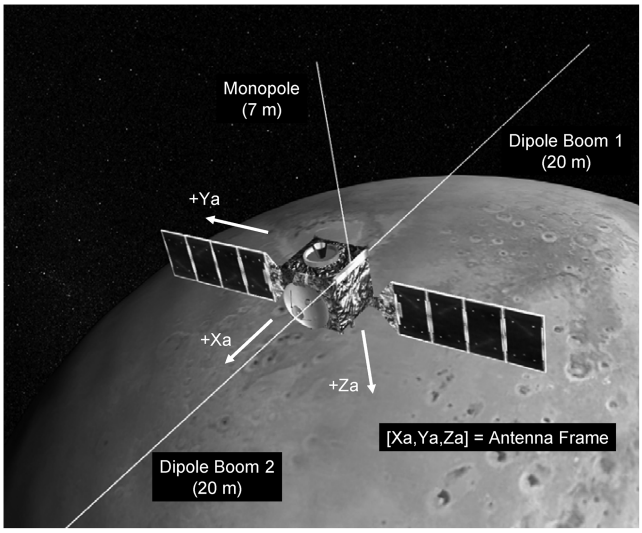

Fig. 2 Three deployed MARSIS booms and reference antenna coordinate system.

II. Dipole Boom 1 Deployment

The MARSIS deployment was initially scheduled for 20 April 2004, but was delayed after the discovery that the original analysis had underestimated the deployment dynamics. Over the course of the following year, an intense testing and analysis effort was undertaken that focused on more accurately quantifying the boom properties, validating the deployment model, and assessing any risk posed to the health of the Mars Express spacecraft. Component tests were done on the hinges to better quantify their deployment torque, buckling strength, and postbuckling behavior. Results obtained from the component tests were ultimately responsible for the successful deployment of the MARSIS booms [2,3].

Dipole boom 1 was deployed on 4 May 2005, after which the spacecraft recovered from its post deployment attitude and was stable. However, telemetry returned from the spacecraft indicated two anomalies in the deployment: first, the deployment dynamics were outside of the Monte Carlo simulation results [2], and second, the spacecraft inertia and measured structural natural frequencies both indicated that the boom had not completely locked into place. Careful correlation between the measured spacecraft inertias and frequencies showed that hinge 10 had stalled at an angle approximately 40 deg from full deployment. Also, the lowest measured natural frequency was 0.043 Hz, which was well below the expected fundamental natural frequency of 0.095 Hz. The latter proved to be a potentially serious problem, as the observed frequency of 0.043 Hz was inside the spacecraft's controller bandwidth of 0.05 Hz.

During the deployment of dipole boom 1, the spacecraft control system was disengaged to prevent interaction of the control system with the uncertain deployment dynamics. The only data measured during the deployment were the spacecraft angular rates (sampled at 8 Hz), which were then used to infer the boom dynamics and its final state. The first 100 s of the flight measured ω_y data are plotted in Fig. 3. As indicated in Fig. 3, the primary observable frequency about the Y axis during the deployment was at ~0.144 Hz, which is significantly different from the expected frequency of ~0.1 Hz. In fact, there were three easily observable frequencies (and later, a fourth) instead of the expected two, as shown in the flexible modes test (using thruster firings) frequency results plotted in Fig. 4. Additionally, the observed damping ζ was approximately 0.6–0.8%, which was well below the lower limit of 2% used in the Monte Carlo analysis; the low damping is attributed to the cold temperature which was below the glass transition temperature of the room temperature vulcanizing silicone used in some of the boom joints. The hinges are numbered sequentially from root to tip, as shown in Fig. 5.

In addition to the unexpected frequencies, an analysis done by the ESA flight dynamics team [4] indicated that the expected change in spacecraft inertia was also not met. To be precise, the changes in the I_{yy} and I_{zz} terms were smaller than expected and the change in the I_{xz} term was positive rather than negative. These differences can be explained if one assumes that a single hinge location was not locked into position, but was instead stalled at an angle such that the outboard portion of the boom was deflected in the positive Z direction. Under these conditions, the hinge angle can be uniquely determined from the known mass distribution of the boom and the measured change in inertia where only a small number of hinges provide realizable angles. The precise hinge location could not be determined from the measured inertia changes alone due to

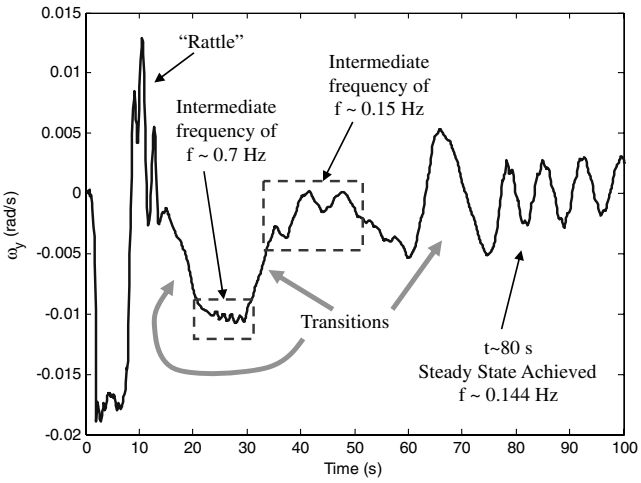

Fig. 3 Spacecraft ω_y for the first 100 s following the dipole boom 1 deployment shows several observable intermediate frequencies that likely indicate partially locked boom segments. There were at least four individual hinge locking or buckling events following the initial deployment phase (including hinge 10).

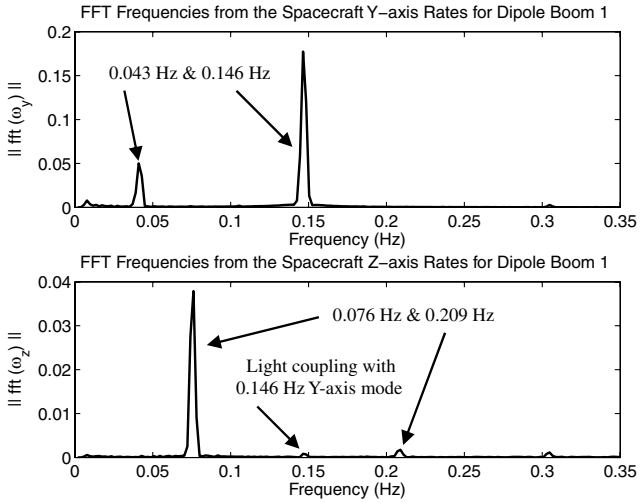

Fig. 4 Dipole boom 1 measured structural frequencies following the initial deployment. These results are from the first spacecraft thruster firing test to measure the flexible modes.

limitations on the measurement resolution, but the most feasible candidates were identified as hinges 9, 10, and 11.

In an effort concurrent with the inertia measurements, the boom was modeled in NASTRAN using different assumed hinge locations and angles in an attempt to match the observed frequencies. By controlling the hinge stiffness and stall angle, it was a relatively straightforward operation to uniquely match the three lowest observed frequencies for each candidate stalled hinge location, leaving little doubt of the boom geometry. This was accomplished by varying the hinge angle and bending stiffness in the plane of deployment to match the two observed f_y frequencies and then varying the out-of-plane stiffness to match the lowest observed f_z frequency.

Only the first three modes were used in the original model tuning, but the analysis results also later confirmed a fourth observable frequency at 0.209 Hz, which is identified in Fig. 4. The corresponding first four mode shapes from this analysis are shown in Fig. 6. The hinge location itself is the fourth degree of freedom that allows the fourth mode to be matched. Results from this study are summarized in Table 1. Using all four frequencies uniquely identifies the hinge location and angle, but the fourth frequency was not trusted until the hinge angle was confirmed by comparison to the inertia measurement results.

By correlating the results from the NASTRAN study with separate measurements of the spacecraft inertia, it was determined that the only case that uniquely matched both the inertia and frequency observations was that of hinge 10 stalled at an angle of 40 deg relative to the X axis, with the tip deflected in the $+Z$ direction in the X–Z plane. No other single location and geometry combination could duplicate the simultaneous match provided by this simple stalled hinge 10 model. Not only was the hinge position determined, but the

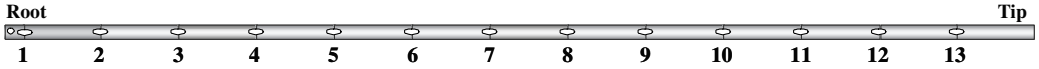

Fig. 5 Dipole boom geometry with hinges numbered in increasing order from the root to the tip.

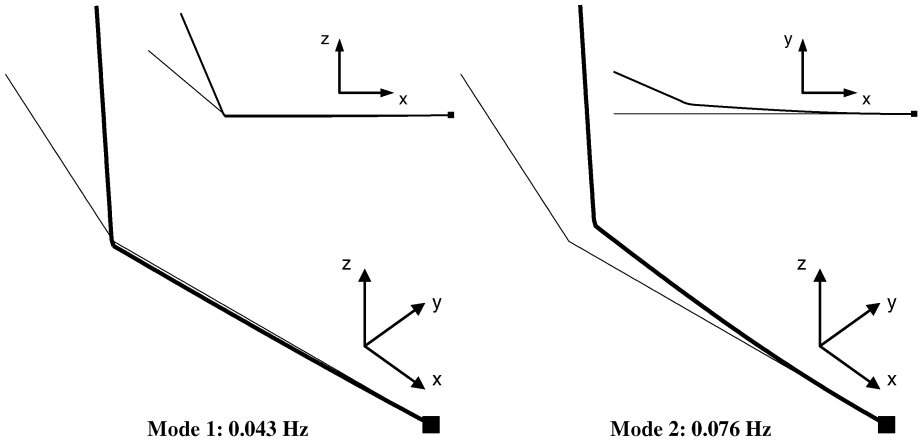

Fig. 6 NASTRAN mode shapes 1–4 for the partially deployed dipole boom 1 with hinge 10 stalled at 40 deg.

Table 1 Results from the NASTRAN study used to help determine the boom 1 state

Hinge number	Hinge angle	$(f_y)_1$, Hz	$(f_z)_1$, Hz	$(f_y)_2$, Hz	$(f_z)_2$, Hz
9	65 deg	0.043	0.076	0.146	0.226
10	40 deg	0.043	0.076	0.146	0.209
11	15 deg	0.043	0.076	0.144	0.183
Measured	?	**0.043**	**0.076**	**0.146**	**0.209**

error in the hinge angle was estimated to be only ±5 deg. These results were corroborated by the verification of the fourth observable boom frequency at 0.209 Hz. Given the close correlation to both the measured frequency and inertia properties, plans to explore multiple stalled hinge locations were abandoned.

III. Dipole Boom 1 Anomaly Resolution

One important observation made during the hinge torque profile testing [2] was that the MARSIS hinge has a secondary stability or a stall point where the opening torque goes to zero at approximately 50 deg from the desired straight geometry. This test result also matched well with the flight analysis, leaving little doubt as to the boom's geometry. The average hinge torque curve developed from the component testing for use in the Automatic Dynamic Analysis of Mechanical Systems (ADAMS) simulation of the deployment is shown in Fig. 7 and illustrates this behavior. This stalling phenomenon was determined in testing to be a strong function of temperature and disappears as the hinge is warmed from its flightlike temperature of −70°C to room temperature of 20°C. It is also possible that aging effects could have further exacerbated the problem, given the long-term vacuum exposure and multiple aerobraking thermal cycles. Lenticular hinges are known to have highly nonlinear torque responses [2,5], but a temperature-dependent stalling torque has not been extensively studied.

Evaluation of the flight attitude and boom geometry indicated that the partially deployed hinge 10 was in the shadow of the straight root portion of the boom, as illustrated in case 1 of Fig. 8. Thermal analysis later showed the hinge in this configuration to be very cold, with portions of the modeled hinge having temperatures below −140°C. Although its threshold temperature was never measured, in every case tested and with no stimulus other than raising its temperature, a stalled hinge was always observed to lock into place as it warmed from its cold test temperature. The expansion of the warm side and contraction of the cold side of the hinge also acted to retard its opening motion to a certain degree, but this was found through the analysis to be a second-order effect.

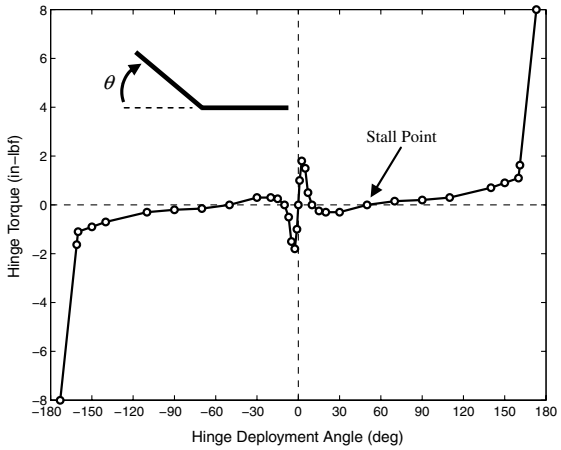

Fig. 7 Average hinge deployment torque profile at −70°C. Note the onset of negative torque at ∼50 deg that can lead to a stall condition for low rates. The artificially steep slope near 180 deg is intended to prevent hinge self-penetration.

After it was conclusively determined that hinge 10 was stalled at a 40 deg angle, and given the known temperature dependence of the stall characteristic, a possible solution was proposed to help the stalled hinge to deploy. The sun incidence angle on hinge 10 after its initial deployment was very low and the hinge was partially in the shadow of the root section itself, as shown in case 1 of Fig. 8. Although this was not the situation during the deployment, the timescale of those dynamics was too short for the sun to adequately warm the hinges, and the final geometry prevented hinge 10 from warming above its deployment temperature. In fact, the deployment dynamics were so energetic that the likelihood of an incomplete hinge deployment was considered to be very low before this experience in flight.

Once the partially deployed boom 1 geometry was determined, a maneuver was performed to reorient the spacecraft to provide optimal illumination of the interior of the stalled hinge elbow, as shown in case 2 of Fig. 8. It was hoped that the solar illumination would be sufficient to raise the temperature of the hinge above the stall threshold temperature, where the secondary stability point vanishes. A more aggressive set of maneuvers involving an escalating number of thruster pulses to help excite the boom was also planned, in the event that temperature alone was not enough. The illumination maneuver was performed on 10 May 2005, and flight data showed that, after a hold time of approximately 5 min, hinge 10 fully deployed and locked into place. The spacecraft was 123 million miles from Earth when it encountered a stalled deployment of a hinge located 15 m from the spacecraft, with no direct mechanical means to actuate the hinge, and the only sensors available were the spacecraft rate gyros. Despite these circumstances, the team was able to precisely determine the boom geometry and, based on results from ground tests of component hinges, to correct it with a simple attitude maneuver.

Thermal analysis done following the boom 1 lockout, in preparation for the boom 2 deployment, indicated that the temperature before the maneuver was indeed very cold, as shown in Fig. 9. Following the maneuver, the temperature on the inner side of the hinge approached a steady-state value near 0°C, as shown in Fig. 10. The spacecraft measured ω_y during the case 2 maneuver, attitude hold, and subsequent hinge 10 lockout are shown in Fig. 11. The final measured frequencies and changes in spacecraft inertia, indicating that boom 1 was indeed successfully and fully deployed, are shown in Fig. 12 and summarized in Table 2, respectively.

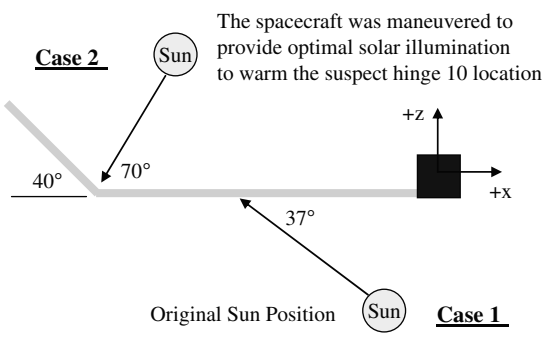

Fig. 8 Case 1 shows the sun illumination of boom 1 following its initial deployment. Case 2 shows the relative sun position and illumination used to warm hinge 10 leading to its lockout and successful deployment of boom 1.

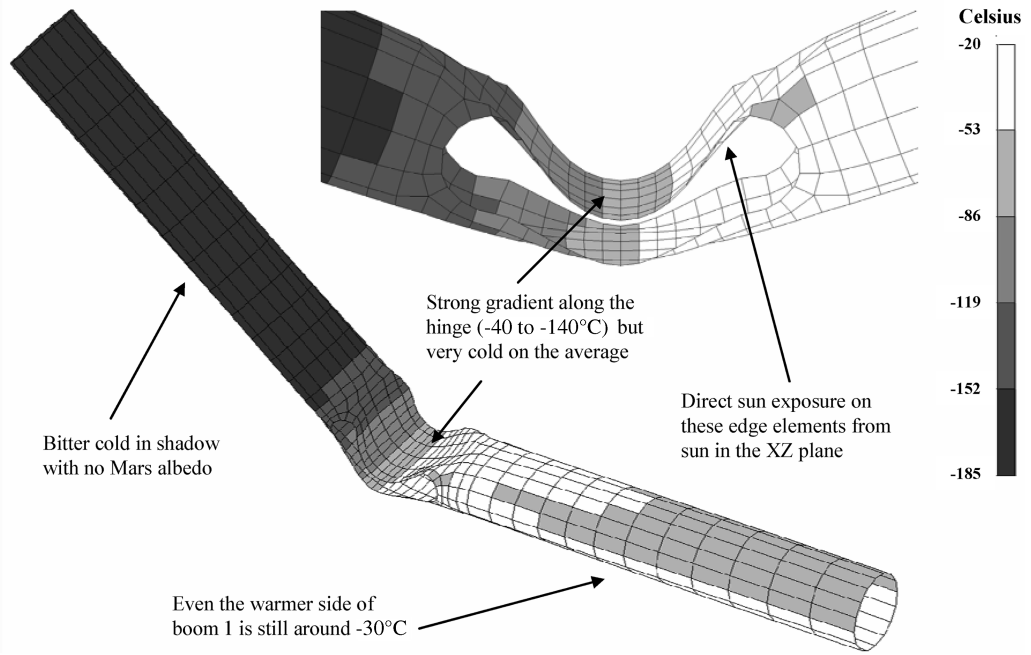

Fig. 9 Radiative thermal analysis of the stalled hinge 10 during the case 1 orientation from Fig. 8, characteristic of the spacecraft's controlled attitude following the boom 1 deployment.

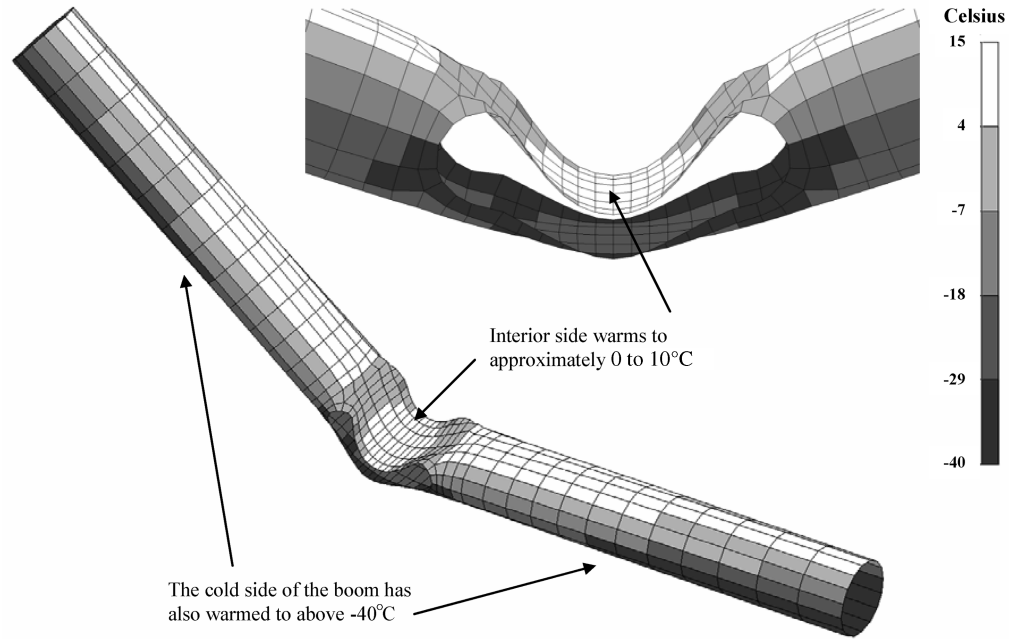

Fig. 10 Radiative thermal analysis of the stalled hinge 10 during the case 2 orientation from Fig. 8 warming maneuver that led to the complete deployment of boom 1.

IV. Dipole Boom 2 Deployment

In light of the experience gained from the dipole boom 1 deployment, a number of potential mitigating actions were recommended to help increase the probability of the second dipole boom deploying successfully. These included the following:

1) Cancel the previously planned shading maneuver, which was originally designed to remove energy from the deployment.

2) Leave the printed circuit board heaters turned on and at their warmest nominal setting.

3) Maintain solar illumination of the external hinges before deployment.

4) The coldest (even-numbered) hinges should receive the maximum possible solar flux on their inner (folded) side as soon as practical after deployment.

There were three additional actions that were considered but rejected. First, it was found that the Mars albedo could significantly affect the boom temperature once it was deployed, however, it was determined that it was infeasible to take advantage of this effect due to spacecraft operational and time-line restrictions. Second, it was noted that orienting the spacecraft to illuminate the now-vacant boom 1 cavity may help to increase the temperature of the interior (even-numbered) hinges, but this effect was shown to be of minimal benefit and would have introduced additional unknowns and more complicated maneuvers. And third, a maneuver was considered that would have spun-up the spacecraft in an attempt to enhance the likelihood of the boom reaching its full deployment through the additional centripetal acceleration; however, it was determined that this would not alter the direction of the deployment and would only

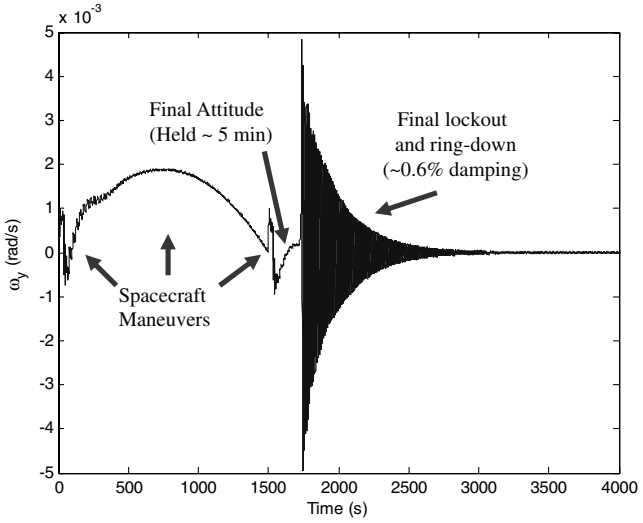

Fig. 11 Measured spacecraft ω_y during the case 2 maneuver to warm the interior of hinge 10 leading to its final lockout and successful deployment of boom 1.

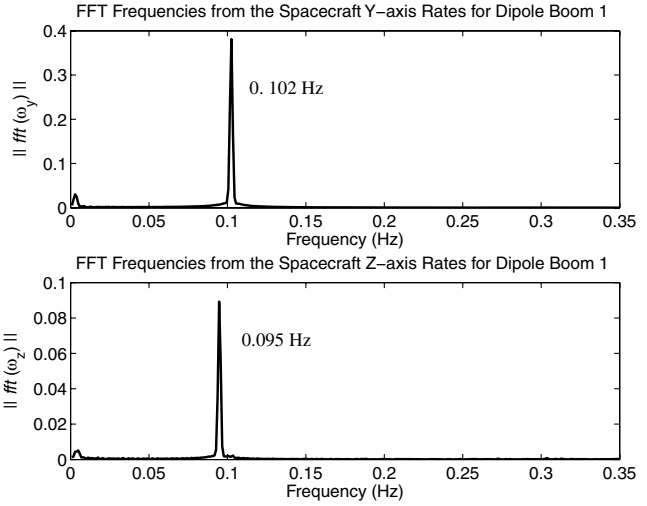

Fig. 12 Dipole boom 1 measured structural frequencies following the hinge 10 lockout.

add a curvature component to the boom while it unfurled, as its linear momentum was fixed by the initial deployment and would be ineffective. Stated differently, because the boom was flexible in its initial state, the boom would only have the angular momentum remaining from its stowed state and would not pick up the centripetal acceleration until much later in the deployment. Further, the angular rates required to generate significant centripetal accelerations were too high for consideration.

Based on experience from the boom 1 deployment, a slowly rotating or "pirouette" spacecraft maneuver was designed to ensure that, if a similar stall occurred on the coldest (even-numbered) hinges, they would be warmed in a similar fashion before the activation of the spacecraft controller and minimize any additional risk to the spacecraft. This maneuver, diagrammed in Fig. 13, was constrained by Mars Express thermal requirements to limit solar exposure of the star scanners that are mounted on the $-X$ side of the spacecraft. The original procedure had called for orienting the spacecraft to place boom 2 in shadow before deployment to minimize its deployment energy. This maneuver was canceled due to the temperature sensitivity of the hinges.

Unfortunately, it was not possible to simultaneously warm both the odd- and even-numbered hinges before deployment, as they were on opposite sides of the cradle. Also, the even-numbered hinges were "interior" hinges (inside the closed cradle), as shown in Fig. 1, and were much more difficult to warm using solar illumination. The decision was made to warm the odd-numbered hinges to ensure that the root hinge would lock into place. One of the most serious risks was the possibility that a hinge closer to the spacecraft could stall, which would produce a low-frequency mode that also had a high effective mass near 0.02 Hz. A combination such as this could have potentially crippled the spacecraft's controller.

To guard against a potential even-numbered (and possibly odd-numbered) hinge stall, the spacecraft was configured to achieve an average spin rate of $+0.1$ deg /s about the spacecraft Y axis before the deployment command. This was accomplished by off-loading the reaction wheels, until the correct angular momentum required to produce the average spin rate was stored in them, such that, when the controller was disabled at the beginning of the deployment, the uncontrolled reaction wheels would spin down and generate the desired motion. The full maneuver was performed over a 30 min period. A time-varying thermal model of an even-numbered hinge was analyzed to confirm that the pirouette maneuver would raise the hinge temperatures to a level similar to what was achieved on boom 1, hinge 10 during the first warming maneuver. Temperature results for the nodes along the boom centerline obtained from this analysis are compared with the steady-state temperatures from the first maneuver in Fig. 14. These results indicated that, even in the event of another stalled hinge, the spacecraft should rotate the hinge through an attitude that would warm it enough to fully deploy before the reengagement of the spacecraft control system.

The deployment of dipole boom 2 was initiated on 14 June 2005 and generated exactly the expected resonant frequencies and changes to the spacecraft inertia. The resulting flight ω_y data recorded during the deployment are plotted in Fig. 15 with some annotation. As anticipated, the deployment of boom 2 excited the flexible modes of boom 1, which are then present throughout the collected data; hence, it is very difficult to make any meaningful conclusions regarding the boom 2 deployment dynamics. In retrospect, the MARSIS team was very fortunate that the stalled hinge occurred on the first boom and not the second boom, as the two booms have a strong interaction with

Table 2 Comparison of expected and measured frequencies and changes in spacecraft inertia tensor (flexible modes are listed according to the axis about which their motion is sensed)

	Expected	After initial deployment	After hinge 10 lockout
Change in spacecraft inertia:	$\begin{bmatrix} 0 & -9 & -5 \\ -9 & +139 & 0 \\ -5 & 0 & +139 \end{bmatrix}$	$\begin{bmatrix} 0 & -11 & \mathbf{+6} \\ -11 & \mathbf{+132} & +1 \\ \mathbf{+6} & +1 & \mathbf{+132} \end{bmatrix}$[a]	$\begin{bmatrix} -4 & -11 & -2 \\ -11 & +138 & +1 \\ -2 & +1 & +139 \end{bmatrix}$
Damping:	3.5%	<1.0%	<1.0%
Flexible modes:	x none $y \sim 0.1$ Hz $z \sim 0.1$ Hz	x none y 0.043 Hz[b] y 0.146 Hz z 0.076 Hz z 0.209 Hz	x none y 0.102 Hz z 0.095 Hz

[a]ΔI_{xz} has wrong sign, ΔI_{yy} and ΔI_{zz} < expected.
[b]The 0.043 Hz mode was also excited by eclipse and solar array rotations.

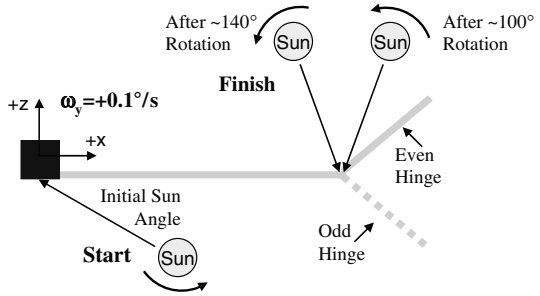

Fig. 13 Spacecraft pirouette slew maneuver used during the dipole boom 2 deployment. The maneuver was designed with a primary goal to illuminate the interior of an even-numbered hinge should one stall. Thermal analysis also showed that perpendicular illumination of the back of an odd-numbered hinge resulted in moderate warming with a significant chance that a stalled odd-numbered hinge might be unfrozen as well.

each other and it may have been much more difficult to determine the stall geometry were it to have occurred on the second boom deployment. At the very least, a stalled hinge on the second boom would have reduced the certainty of the judgments made in the analysis.

The 7-m monopole boom was deployed on 17 June 2005, also without incident. Unfortunately, due to its very low mass and inertia, the final state of the monopole is currently uncertain and may never be known (the radar also cannot be used to check its geometry), but it was determined not to present a risk to the spacecraft, regardless of its final state.

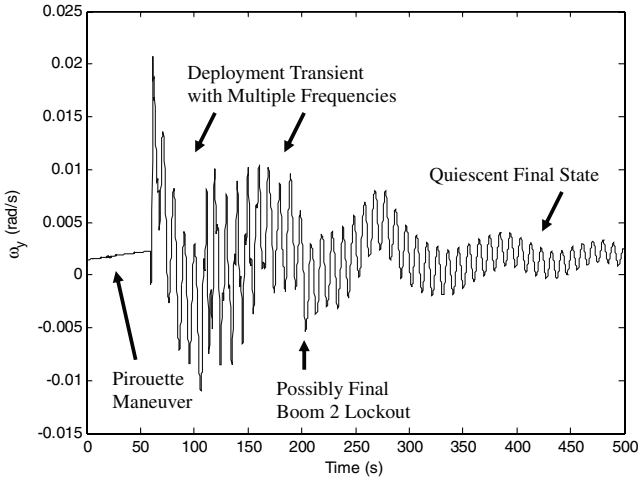

Fig. 15 Measured spacecraft ω_y during the dipole boom 2 deployment. Note that boom 1 is excited at the onset and rings throughout the boom 2 deployment.

A comparison between the flight measured modal frequencies and the NASTRAN modeled frequencies for the final deployed configuration (illustrated in Fig. 2) is given in Table 3. The deployed boom stiffness properties in the NASTRAN model were tuned to match the deployed frequencies measured after dipole boom 1 locked into place. Note that the lowest frequency drops from 0.095 Hz in Table 2 with only dipole boom 1 deployed to 0.085 Hz in Table 3 with all three instrument booms deployed. The explanation for this is

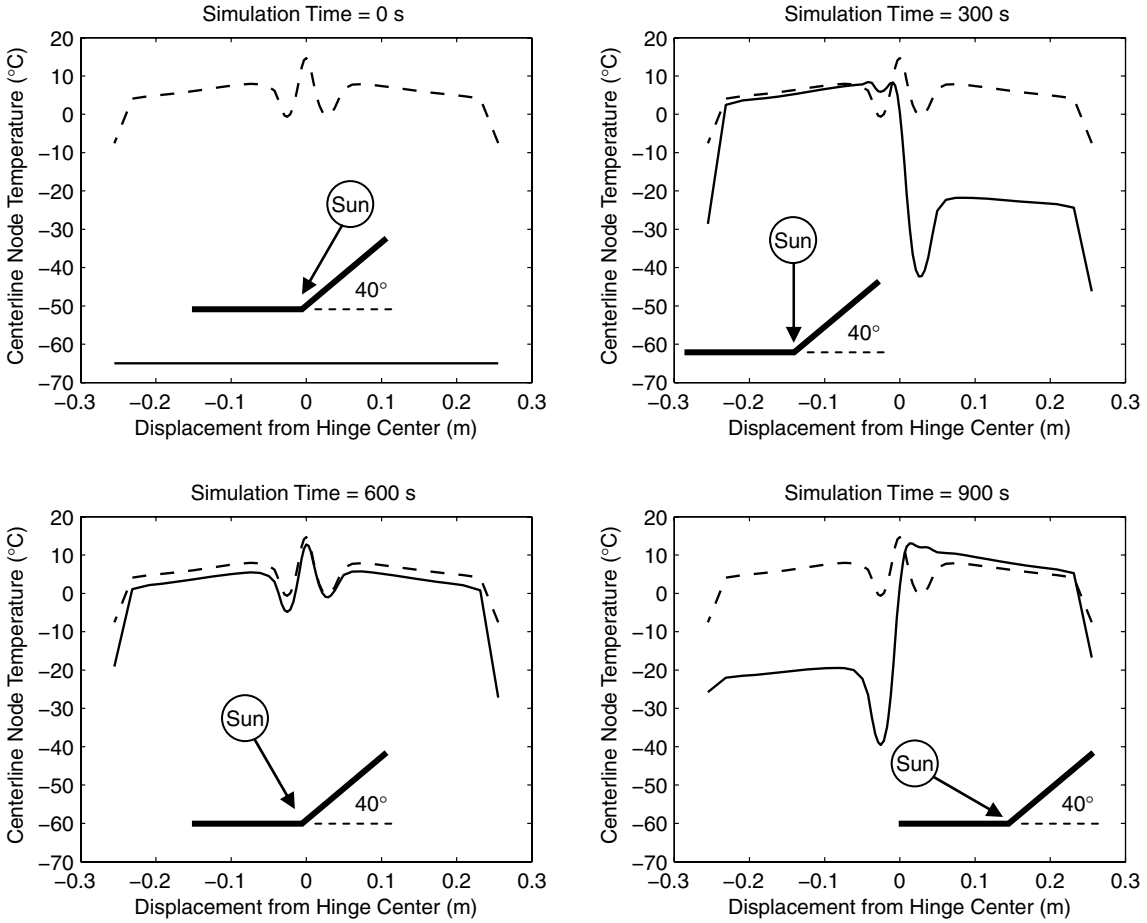

Fig. 14 Centerline node temperatures at 300 s intervals during a simulated pirouette slew maneuver. The orientations are swept in the direction indicated in Fig. 13, with temperatures calculated for an even-numbered hinge stalled at 40 deg from full deployment. The results from the static orientation used for hinge 10 of boom 1 with a symmetric heating of the hinge interior are shown as the dashed line and represent the limiting case for an infinite hold time. The initial boom temperature at $t = 0$ was assigned to be −65°C.

Table 3 Comparison between flight measured flexible mode frequencies and NASTRAN model results following the third boom deployment

Mode number	Predicted freq., Hz	Measured freq., Hz	Difference, Hz	Sensing *X* axis	Sensing *Y* axis	Sensing *Z* axis
1	0.086	0.085[a]	N/A		Symm.	
2	0.089					Symm.
3	0.100	0.100	0			Asymm.
4	0.115	0.115	0		Asymm.	
5	0.355	——	——	Asymm.		
6	0.357	——	——		Asymm.	
7	0.541	——	——		Symm.	
8	0.547	0.54	−0.007		Asymm.	
9	0.558	——	——			Symm.
10	0.560	0.56	0			Asymm.

[a]Cross-talk sensing through *Y* axis and *Z* axis.

that a single boom acts to rotate the spacecraft at its cantilevered root, whereas the opposing dipole booms act to translate the spacecraft without rotation when the booms deform symmetrically. Therefore, the fully deployed state is closer to a fixed boundary condition and has a corresponding lower frequency.

The correlation to flight data is excellent with only tiny discrepancies in frequency. Modes 1 and 2 are symmetric with respect to the *Y* and *Z* axes and couple with each other about the *X* axis. Nevertheless, a single frequency peak was still detectable due to their offset location with respect to the spacecraft c.g., which resulted in rotation about the *X* axis; for example, if the spacecraft translates along the *Z* axis, because the booms lie on the negative *Y* axis, the motion will generate a moment about the *X* axis. Similarly, a spacecraft motion along the *Y* axis will also generate a moment about the *X* axis. Hence, the fundamental symmetric modes are coupled and are not easily visible on the *Y* or *Z* axes. Note that the prelaunch fixed-base predicted frequencies for modes 1 and 2 were 0.078 Hz and 0.081 Hz, which are very close to the measured flight frequencies in Table 3 of $\sim$0.085 Hz due to the free–free mode of the spacecraft. All of the other asymmetric modes were detectable up to the 10th flexible mode, with the exception of the monopole modes (5 and 6) which had too little effective mass to be observed.

V. Conclusions

There are a number of important characteristics that govern the behavior of a lenticular (carpenter tape) structure and these must each be measured and accounted for in planning for its deployment. These include, but are not limited to, material selection, hinge construction, temperature sensitivity, long-term aging, and total stowed energy. Unfortunately, it is not possible to perform a meaningful full-system test on the ground, and so an accurate component model of the boom is extremely important.

Deployments of this type also need to consider the sensitivities of the spacecraft and include a very conservative estimate of the dynamic deployment envelope. A failure modes analysis should be conducted with particular attention paid to the interaction with the spacecraft control system. MARSIS was rather unique in that the antenna deployments roughly doubled the spacecraft inertia about the *Y* axis. Other spacecraft may not see this level of change or this large of an effective mass at such a low frequency, but care must be taken nonetheless to guard against any eventualities.

Acknowledgments

The authors would like to acknowledge the hard work and thorough analysis of the ESA and European Aeronautic Defence and Space Company Astrium engineering and flight team, and wish to recognize Michael Saeger, Raymond Becker, and Mike Fedyk for their timely assistance in performing the hinge thermal modeling. The research described in this paper was carried out at Northrop Grumman Space Technology Astro Aerospace (Contract No. 1263269) and at the Jet Propulsion Laboratory, California Institute of Technology, under a contract with NASA.

References

[1] Marks, G. W., Reilly, M. T., and Huff, R. L., "The Lightweight Deployable Antenna for the MARSIS Experiment on the Mars Express Spacecraft," *36th Aerospace Mechanisms Symposium*, NASA CP 2002-211506, Apr. 2002, pp. 183–196.

[2] Mobrem, M., and Adams, D. S., "Deployment Analysis of Lenticular Jointed Antennas Onboard the Mars Express Spacecraft," *Journal of Spacecraft and Rockets*, Vol. 46, No. 2, 2009, pp. 394–402. 10.2514/1.36890

[3] Adams, D. S., Mobrem, M., and Sabahi, D., "MARSIS Antenna Deployment Testing and Analysis," *Spacecraft and Launch Vehicle Dynamic Environments Workshop*, Aerospace Corp., El Segundo, CA, June 2005, http://www.aero.org/conferences/sclv/2005proceedings.html.

[4] Denis, M., Moorhouse, A., Smith, A., McKay, M., Fischer, J., Jayaraman, P., Mounzer, Z., Schmidt, R., Reddy, J., Ecale, E., Horttor, R., Adams, D., and Flamini, E., "Deployment of the MARSIS Radar Antennas On-Board Mars Express," 9th International Conference on Space Operations, AIAA Paper 2006-5959, 2006.

[5] Seffen, K. A., and Pellegrino, S., "Deployment Dynamics of Tape Springs," *Proceedings of the Royal Society of London A*, Vol. 455, No. 1983, Mar. 1999, pp. 1003–1048.

L. Peterson
Associate Editor